https://doi.org/10.2352/ISSN.2169-4451.2017.32.424

Novel Approach for Predicting Coffee-Ring-Effect in Drying Droplets Based on Binary Solvent Mixtures from Substance Data

Danny Lehmann, Hauke H. Langner, Vico Haverkamp, Klaus Krüger; Helmut-Schmidt-University/University of the Federal Armed Forces Hamburg, Holstenhofweg 85, 22043 Hamburg, Germany

Abstract

In this study we present a novel approach using dimensionless numbers that allows for the prediction of ring-like structures in drying ink drops based on binary solvent mixtures by substance data. Mechanisms considered in this approach are suppression of Marangoni-flows due to fast evaporation times as well as the potential strength of Marangoni-flows. The proposed approach is validated experimentally. Single spots based on various solvent compositions are inkjet-printed and characterized with respect to the structure by means of microscopy.

Introduction

Inkjet printing as manufacturing process for functional structures is subject of research since the end of the 1980's [1]. Fabricating components, inkjet printing is appropriate for a variety of applications, e.g. passive electronic components, LEDs, RFID transponders, sensors or applications in biotechnology [2], [3].

The functional material is dispersed in a carrier fluid in the form of nano particles. In general, particle loaded inks based on organic solvents are applied in functional inkjet printing. While drying on a non-absorbing substrate, a particle loaded droplet is subject to fluid mechanical effects. These effects arise from the evaporation and the surface tension of the solvent as well as from the interaction between ink and substrate.

With respect to the coffee-ring-effect (CRE), a flow develops in the drying droplet; particles are carried towards the edge. As a result, particles are distributed inhomogeneously on the substrate. The governing mechanisms were first described by Deegan et. al. in 1997 [4]. Furthermore, temperature and concentration gradients can initiate a Marangoni-flow in the drying droplet [5]. If both effects appear at the same time, flows are superposed and a complex flow behavior occurs. Under certain conditions, the inhomogeneous distribution of particles due to CRE can be compensated by Marangoni-flow [6].

To investigate the stated effects experimentally, the drying process of particle loaded droplets can be observed by high speed cameras. Numerous studies examine single mechanisms regarding the stated phenomena, e.g. [7], [8], [9].

At the Institute of Automation Technology, the formulation of functional inkjet inks as well as applications of functional inkjet printing are researched since 2004. Within the project "Inkjet-printing of photo electrochemical cells", photo active electrodes are structured by CRE in order to increase the free surface for better light capture.

Experimental

The impact of the drying behavior on the structure of inkjet-printed spots is observed. The evaporation of inkjet carrier fluids can be observed with high speed cameras. In this study, we desist from tracing the whole evaporation process. Instead, the distribution of the nano particles on the substrate after complete drying of the printed spots is investigated. Three series of experiments are performed, the examined binary mixtures are listed in table 1.

Table 1*. Investigated binary solvent mixtures, compositions and substrate temperatures*

series	mixture	composition wt.-%	substrate temperature °C
1	BC/DMAc	70:30	40
1	BC/DMAc	70:30	60
1	BC/DMAc	70:30	80
2	BC/DMAc	90:10	60
2	BC/DMAc	70:30	60
3	BC/DEG	50:50	80
3	BC/DEG	70:30	80
3	BC/BUG	50:50	80
3	BC/ISO	50:50	80
3	BC/DMAc	70:30	80
3	BC/DMAc	90:10	80
3	BC/PEN	50:50	80
3	BC	100	80
3	PEN/ISO	50:50	80
3	PEN/EG	50:50	80

First, the impact of substrate temperature on the resulting structure is investigated (series 1). For this purpose, single spots are inkjet-printed with a mono dispenser (MDK-K-140, Microdrop GmbH) on glass substrates (Solaronix SA) at selected temperatures. The temperature at the substrate surface is monitored with a thermometer (80TK thermocouple, Fluke Co.) and is 40, 60 and 80±5 °C. The printed spots are examined by means of digital microscopy (VHX-S15 microscope, Keyence Co.). In addition to microscope photographs, half profiles of the printed spots are prepared from three-dimensional microscope images. These are generated from a series of single microscope images. The binary solvent mixture consists of 70 wt.-% butyl dyglycol (BC) and 30 wt.-% dimethyl acetamid (DMAc). Solids content is 5 wt.-%, TiO_2 particles with a mean diameter of 20 nm are used. The fraction of stabilizing additive ethylcellulose (Dow Chemical Co.) is 2 wt.-%.

With the same experimental setup, the impact of the ink composition is investigated (series 2). Inks based on mixtures of BC and DMAc are printed, the fraction of the latter is 10 and 30 wt.-%. Temperature of the substrate in this series is kept constant at 60 °C. Solids and additive contents are the same as before.

Validating the theoretical approach, further inkjet inks based on binary solvent mixtures are inkjet-printed (series 3). The substrate temperature for all printed inks here is 80 °C, the solid substance content is 5 wt.-% TiO_2 particles with mean diameter of 20 nm. The solvents here are butyl diglycol (BC), diethylene glycol (DEG), butyl glycol (BUG), isopropanol (ISO), dimethyl acetamid (DMAc), 1,5, pentandiol (PEN) and ethylene glycol (EG).

Modeling

The basic notion of the proposed approach is to use dimensionless numbers that are representative for the behavior of the drying spot with respect to the formation of ring-like structures.

The first physical value applied here is the vapor pressure. The vapor pressure of binary mixtures possesses two values, one value for the fluid phase and one value for the vapor phase respectively. In order to obtain a value that allows for a comparison of the different compositions, a combined value $p_{mixture}$ is calculated from the substance data of the pure components assuming a linear relation between the two components:

$$p_{mixture} = c_1 p_1 + c_2 p_2. \quad (1)$$

Here, c_1 and c_2 are the fractions of the two components with respect to the mass; p_1 and p_2 are the vapor pressures of the two components. For the following observations, the vapor pressure is normalized and rendered dimensionless by refering it to the pressure at standard conditions $p_0 = 100$ kPa:

$$p^*_{mixture} = p_{mixture}/p_0. \quad (2)$$

For comparison of the potential strength of the Marangoni-flow, the Marangoni-numbers with respect to thermally driven flow Ma_T and with respect to concentration driven flow Ma_C are used. These dimensionless numbers are commonly used in the field of fluid mechanicas to describe the strength of Marangoni-flows and can be written as follows [10], [11]:

$$Ma_T = (\partial\sigma/\partial T)((L\Delta T)/(\eta a)), \quad (3)$$

$$Ma_C = (\partial\sigma/\partial z)((L^2)/(\eta\delta)), \quad (4)$$

with

$$a = \lambda/(c_p\rho). \quad (5)$$

Here, ΔT is the effective temperature difference, L a characteristic length, η the viscosity, a the thermal diffusity, λ the heat conductivity, c_p the heat capacity, ρ the density, $\partial\sigma/\partial T$ the change of surface tension with respect to the temperature, $\partial\sigma/\partial z$ the change of surface tension with respect to the location and δ the coefficient of diffusion.

The evaporation of fluids on heated substrates is a strongly dynamic process. The temperature and the composition in the drying spot changes with time and is strongly dependent on the location, whereupon the physical values in the equations stated above are dependent on the temperature and the composition of the mixture. The proposed approach neglects the change of physical data during the drying process. Instead, it uses the substance data valid directly after the impact of the droplet on the substrate instead to predict the formation of ring-like structures.

It is assumed that a very short time after impact, the solvent component 1 with the higher vapor pressure has already totally evaporated at the bottom of the spot very close to the substrate. Hence, in this area $c_1 = 0$ and $\sigma = \sigma_2$ apply. The temperature in this area is assumed to be substrate temperature due to strong heat convection at the solid-fluid interface. All substance data is assumed to still have the initial values at the considered moment directly after impact. These initial values depend on the temperature of the impacting droplet which is assumed to be 20 °C and the initial composition according to table 1.

The values for the physical data of binary mixtures used in equations 3 and 4 depend on the composition of the mixture. They are calculated assuming that resulting values depend linear on the composition. So any substance data $X_{mixture}$ of the binary mixture is assumed to be

$$X_{mixture} = c_1 X_1 + c_2 X_2 \quad (6)$$

with the substance data of the pure compounds X_1 and X_2. The most substance data for pure components are taken from literature. The values for heat conductivity and heat capacity of pure substances as well as the coefficient of diffusion for the mixture are calculated with quantitative equations according to [12], which allow for aproximately calculating substance data from chemical formula of the substance. The change of surface tension with respect to the temperature $\partial\sigma/\partial T$ can be calculated from Eötvös rule [13], [14]. For the characteristic length L, the geodetic distance from the substrate to the center of the spot is chosen. This length can be calculated from the contact angle of the spot on the substrate. Values for the latter were measured and will be published in [15]. By this definition, a significant value for the change of surface tension along the surface can be calculated for the mixture by assuming a linear correlation:

$$\partial\sigma/\partial z = (\sigma_{mixture} - \sigma_2)/L, \quad (7)$$

where σ_2 is the component with the lower vapor pressure.

The influence of the solids content on the substance data is neglected, because the value of 5 wt.-% is low and kept constant for all investigated mixtures. The influence of the stabilizing additive is considered to be low and also neglected.

It is assumed, that the forming of ring-like structures in binary solvent mixtures can be predicted by evaporation time and the potential strength of Marangoni-flow. For this purpose, the potential strength of Marangoni-flow is plotted against evaporation time. The resulting diagram is divided into three regions. This can be seen in figure 1.

***Figure 1**. Regions with respect to occurrence of ring-like structures*

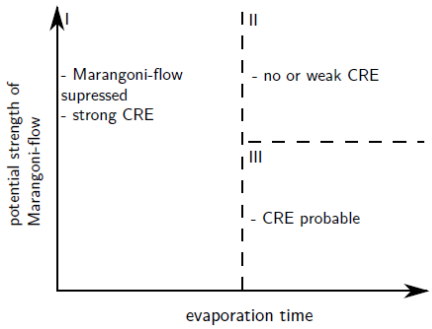

In literature it is shown, that Marangoni-flows are often suppressed at fast evaporation times, because any particle transport due to Marangoni-flow would take more time than evaporation [16]. Hence, in region I it is expected that a distinct ring-like structure appears. If the evaporation is slow, a Marangni-flow can occur. It is assumed, that the possibility for a ring-like structure rises with decreasing potential strength of the Marangoni-flow. Hence, in region III a ring-like structure is also expected. In region II it is expected to have no or weaker ring-like structures due to increasing strength of superposed Marangoni-flow.

Furthermore, it is assumed that evaporation time correlates with the normalized vapor as pressure stated above and the potential strength of Marangoni-flow correlates with the Marangoni-numbers.

Results and Discussion

Temperature and concentration dependence

In figure 2, microscopy images as well as half profiles of the printed spots of series 1 are shown.

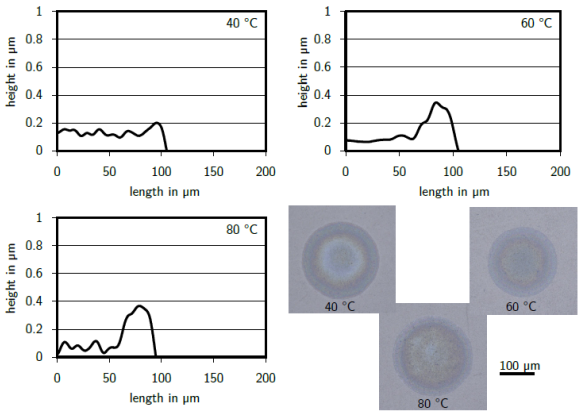

***Figure 2**. Microscopic images and half profiles of inkjet-printed spots based on BC/DMAc 70:30; substrate temperatures 40, 60, and 80 °C.*

In the images of all three spots steps in the color gradients are clearly visible. The darker color at the edge indicates an accumulation of particles at the edge due to CRE. This becomes apparent in the half profiles as well, with increasing temperature a ring-like distribution of particles can be observed at low intensity at 40 °C and at strong intensity at 60 and 80 °C.

The ink used here generally fulfills the condition for occurance of CRE according to [4]. A possible explanation for the behavior with respect to the more distinct ring-structure at elevated temperatures can be found in a Marangoni-flow. A Marangini-flow can be developed here due to the temperature difference between substrate and ambient air and due to a concentration gradient. However, as stated above, the possible strength of such a CRE-counteracting Marangoni flow is higher at slow evaporation times, which seems to be the case at the lowest substrate temperature considered in this experiment. The formation of a distinct ring-like structure due to CRE is therefore notably hindered by a Marangoni flow only at 40 °C here. So the leveled substrate temperature might be an explanation for the observed behavior.

The diameter of the spots tends to decrease with increasing substrate temperature. This probably results from the increased ratio of the evaporation time with free contact line and the total evaporation time, which can lead to smaller diameters.

In figure 3, microscopy images as well as half profiles of the printed spots of series 2 are shown.

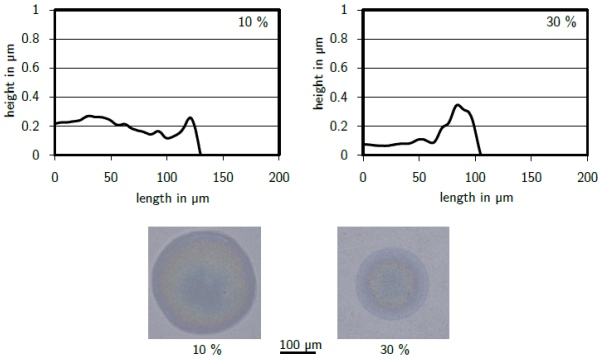

***Figure 3**. Microscopic images and half profiles of inkjet-printed spots based on BC/DMAc at a substrate temperature of 60 °C; compositions 10 and 30 wt.-% DMAc.*

Again, steps in the color gradient are visible in both images, whereat the half profiles indicate a more distinct ring-like structure for the 30 wt.-% DMAc mixture. As described above, the supression of a Marangoni-flow at leveled evaporation times can be used as explanation for the increased accumulation of particles in the right figure. Here, the vapor pressure of the mixture rises significantly due to the higher content of DMAc and hence the evaporation time is shorter. The smaller spot diameter as well as the smaller area of the profile result from the change of evaporation characteristic due to higher vapor pressure as well as from a change of droplet volume due to changed viscosity und subsequently adapted driving voltage in the printing process.

Verification of the proposed approach

First, the printed spots of the tested mixtures of series 3 are classified in three groups according to the microscope images and half profiles: strong CRE, weak CRE and no CRE. Afterwards, the dimensionless numbers according to the equations stated above are calculated for each tested mixture. Table 2 shows the results for the classification of the printed spots, for the calculation of the normalized vapor pressure as well as for the calculation of the Marangoni-number with respect to concentration-driven flows.

***Table 2**. Results of the classification of tested mixtures, of the calculation of the Normalized vapor pressure and of the Marangoni-number with respect to concentration-driven flow.*

mixture	CRE	p^*_{mixture} 10^{-3}	L mm	η mPa s	δ 10^{-12}m^2/s	$\partial\sigma/\partial z$ N/m^2	Ma_C 10^3
BC/DEG 50:50	none	0,023	0,101	21,2	349	69,0	95,5
BC/DEG 70:30	weak	0,022	0,115	15,3	349	36,6	89,8
BC/BUG 50:50	none	0,595	0,135	4,75	367	14,8	154
BC/ISO 50:50	strong	21,5	0,135	4,20	598	33,4	241,5
BC/DMAc 70:30	strong	1,004	0,114	4,82	400	10,5	71,2
BC/DMAc 90:10	weak	0,348	0,128	5,95	400	3,12	21,5
BC/PEN 50:50	none	0,015	0,101	58,2	14,0	64,3	804
BC*	strong	0,020	0,135	6,50	-	0	-
PEN/ISO 50:50	strong	21,5	0,101	55,9	28,3	108,9	700
PEN/EG 50:50	strong	0,040	0,067	65,5	22,9	37,0	112

The microscope pictures and half profiles for the spots examined in series 3 will be published in [15]. The ink based on pure BC is examined in order to compare the carrier fluids based on mixtures with carrier fluids based on pure substances. A value for Ma_C cannot be calculated because there is no coefficient of diffusion and the change of surface tension with respect to the location becomes zero. Table 3 shows the calculation of the Marangoni-number with respect to thermally driven flows.

***Table 3**. Results of the calculation of the Marangoni-number with respect to thermal-driven flow.*

mixture	L mm	η mPa s	ρ kg/m^3	c_p J/(kg K)	λ W/(m K)	ΔT K	$\partial\sigma/\partial T$ µN/(m K)	Ma_T -
BC/DEG 50:50	0,101	21,2	1035	2225	0,153	60	94,3	406
BC/DEG 70:30	0,115	15,3	1002	2175	0,153	60	86,6	542
BC/BUG 50:50	0,135	4,75	927	2207	0,158	60	73,2	1614
BC/ISO 50:50	0,135	4,20	866	2318	0,162	60	86,3	2061
BC/DMAc 70:30	0,114	4,82	949	1920	0,156	60	88,2	1467
BC/DMAc 90:10	0,128	5,95	952	2040	0,159	60	79,5	1252
BC/PEN 50:50	0,101	58,2	976	2200	0,153	60	86,6	126
BC	0,135	6,50	953	2100	0,161	60	75,2	1162
PEN/ISO 50:50	0,101	55,9	889	2418	0,154	60	97,8	148
PEN/EG 50:50	0,067	65,5	1056	2341	0,150	60	117	119

The calculated values shown in table 2 and table 3 are plotted in a diagram as introduced in figure 1. As dimensionless value for potential strenght of Marangoni-flow the product of Ma_T and Ma_C is considered. This value is charged on the axis of ordinate in the diagram. The Ma_C -value for the purely BC-based ink is set to 1.

Temperature is 80 °C in all experiments. Hence, the main impact on evaporation here is expected to arise from the vapor pressure. As the evaporation time decreases with increasing vapor pressure, the reciprocal value of $p^*_{mixture}$, $1/p^*_{mixture}$, is charged on the axis of abscissae in the diagram. The diagram is shown in figure 4.

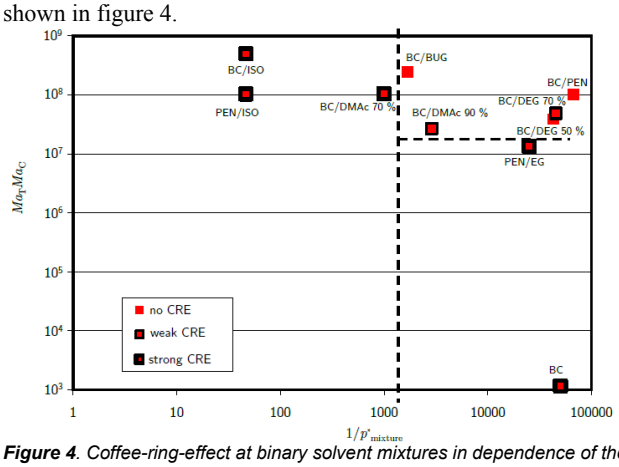

***Figure 4**. Coffee-ring-effect at binary solvent mixtures in dependence of the vapor pressure and the potential strength of Marangoni-flow on glass substrate at a substrate temperature of 80 °C; dashed line: borders of predicted regions*

Logarithmic scaling is chosen for both axes in order to accommodate the rather large range of values. It is attempted to draw the borders of the three regions according to figure 1. One finds, that for normalized vapor pressures greater than 0.001 a strongly developed ring-like structure is observed due to fast evaporation. For values greater than $13 \cdot 10^7$ no ring-like structure is observed due to strong Marangoni-flow. For inks containing higher amounts of solids and additives than the inks considered in this study, the impacts of solids and additives on the physical values have to be considered for the calculation of the dimensionles numbers

Conclusions

We investigate the forming of ring-like structures in drying ink drops based on binary solvent mixtures and low solid contents. First, we show the general behavior with respect to temperature and composition of selected inks based on materials chosen in this study by means of microscope photographs and three-dimensional microscope images.

Subsequently, a novel appoach for predicting the occurance of ring-like structures is proposed. The approach is based on dimensionless numbers which can represent the general drying behavior. The dimensionless numbers are calculated from substance data that are valid for the moment directly after the impact of the droplet on the substrate. The first considered mechanism is the forming of ring-like structures due to fast evaporation and supression of Marangoni-flow. This mechanism is covered by a normalized vapor pressure. The second considered mechanism is the potential strength of the thermal-driven and the concentration-driven Marangoni-flows. This is covered by the product of the Marangoni-number with respect to thermal driven flows and with respect to concentration driven flows.

Experiments are performed in order to test the proposed approach. By means of microscopy, the occurance of ring-like structures for a set of inkjet inks is observed and classified using three categories. For the examined inks, the dimensionsless numbers are calculated and plotted according to the proposed approach. The results show, that the behavior can be predicted using the proposed approach within certain restrictions. The limits of the predicted regions are identified and validated for the specific glass substrate and substrate temperature 80 °C used in this study.

References

[1] P. Calvert, Chem. Mater, 2001, 13, 3299.

[2] J. Perelaer, P. J. Smith, D. Mager, D. Soltman, S. K. Volkman, V. Subramanian, J. G. Korvink, U. S. Schubert, J. Mater. Chem. 2010, 20, 8446.

[3] A. Sridhar, T. Blaudeck, R. Baumann, Material Matters 2011, 6, 12.

[4] R. Deegan, O. Bakajin, T. F. Dupont, G. Huber, S. R. Nagel, T. A. Witten, Nature, 1997, 389, 827.

[5] V. N. Truskett, K. Stebe, Langmuir, 2003, 19, 8271.

[6] H. Hu, R.G. Larson, J. Phys. Chem. B, 2006, 110, 7090.

[7] W. D. Ristenpart, P. G. Kim, C. Domingues, J. Wan, H. A. Stone, Phys. Rev. Lett., 2007, 99.

[8] T. Lim, S. Han, J. Chung, J. T. Chung, S. Ko, C. P. Grigoropoulos, International Journal of Heat and Mass Transfer, 2009, 52, 431.

[9] E.L. Talbot, A. Berson and C. Bain, Proceedings of the NIP 29, 2013, 307.

[10] J. Straub, A. Weinzierl, M. Zell, Wärme- und Stoffübertragung, 1990, 25, 281.

[11] J. Erz, In-situ Visualisierung von Oberflächendeformationen aufgrund von Marangoni-Konvektion während der Filmtrocknung, PhD.-thesis, 2013, Karlsruher Institut für Technologie, Karlsruhe.

[12] VDI, VDI-Wärmeatlas, 2002, Springer-Verlag, Berlin, Heidelberg.

[13] L. Eötvös, Annalen der Physik, 1886, 236,448.

[14] J. Lennard-Jones, J. Corner, Transactions of the Faraday Society, 1940, 36, 1156.

[15] D. Lehmann, Inkjet-Druckprozess für die Fertigung von Strukturen zur photoaktivierten Wasserspaltung, submitted PhD.-thesis, 2016, Helmut-Schmidt-Universität, Hamburg.

[16] T. Lim, J. Yang, S. Lee, J. Chung, D. Hong, International Journal of Precision Engineering and Manufacturing, 2012, 13, 827.

Author Biography

Danny Lehmann received his Diploma from Technical University Hamburg-Harburg in 2012